Titin strain contributes to the Frank–Starling law of the heart by structural rearrangements of both thin- and thick-filament proteins

Younss Ait-Mou[a,1,2], Karen Hsu[a,b,1,3], Gerrie P. Farman[a,4], Mohit Kumar[a], Marion L. Greaser[c], Thomas C. Irving[b], and Pieter P. de Tombe[a,5]

[a]Department of Cell and Molecular Physiology, Loyola University Chicago, Stritch School of Medicine, Maywood, IL 60153; [b]Department of Biological and Chemical Sciences, Illinois Institute of Technology, Chicago, IL 60616; and [c]Department of Animal Sciences, Muscle Biology Laboratory, University of Wisconsin–Madison, Madison, WI 53706

Edited by J. G. Seidman, Harvard Medical School, Boston, MA, and approved January 12, 2016 (received for review August 21, 2015)

The Frank–Starling mechanism of the heart is due, in part, to modulation of myofilament Ca^{2+} sensitivity by sarcomere length (SL) [length-dependent activation (LDA)]. The molecular mechanism(s) that underlie LDA are unknown. Recent evidence has implicated the giant protein titin in this cellular process, possibly by positioning the myosin head closer to actin. To clarify the role of titin strain in LDA, we isolated myocardium from either WT or homozygous mutant (HM) rats that express a giant splice isoform of titin, and subjected the muscles to stretch from 2.0 to 2.4 μm of SL. Upon stretch, HM compared with WT muscles displayed reduced passive force, twitch force, and myofilament LDA. Time-resolved small-angle X-ray diffraction measurements of WT twitching muscles during diastole revealed stretch-induced increases in the intensity of myosin (M2 and M6) and troponin (Tn3) reflections, as well as a reduction in cross-bridge radial spacing. Independent fluorescent probe analyses in relaxed permeabilized myocytes corroborated these findings. X-ray electron density reconstruction revealed increased mass/ordering in both thick and thin filaments. The SL-dependent changes in structure observed in WT myocardium were absent in HM myocardium. Overall, our results reveal a correlation between titin strain and the Frank–Starling mechanism. The molecular basis underlying this phenomenon appears not to involve interfilament spacing or movement of myosin toward actin but, rather, sarcomere stretch-induced simultaneous structural rearrangements within both thin and thick filaments that correlate with titin strain and myofilament LDA.

myofilament length-dependent activation | small-angle X-ray diffraction | rat | passive force | fluorescent probes

The Frank–Starling law of the heart describes a cardiac regulatory control mechanism that operates on a beat-to-beat basis (1). There is a unique relationship between ventricular end-systolic volume and end-systolic pressure that is determined by cardiac contractility. As a result, ventricular stroke volume is directly proportional to the extent of diastolic filling. In conjunction with heart rate and contractility, the Frank–Starling mechanism constitutes a major determinant of cardiac output. Although the Frank–Starling mechanism has been well established for well over a century, the molecular mechanisms underlying this phenomenon are not resolved (1). At the cellular level, an increase in sarcomere length (SL) results in an immediate increase in twitch force development. Existing data, mostly derived from permeabilized isolated myocardium, strongly support the notion that this phenomenon is due to an increase in the Ca^{2+} responsiveness of the cardiac contractile apparatus, a phenomenon termed "myofilament length-dependent activation" (LDA) (1).

The mechanism by which the mechanical strain signal is transduced by the cardiac sarcomere is not known. We have recently demonstrated that LDA develops within a few milliseconds following a change in SL (2), a finding suggestive of a molecular mechanism caused by strain-dependent mechanical rearrangement of contractile proteins. Moreover, although LDA is a general property of striated muscle, it manifests itself to a much greater extent in cardiac muscle compared with slow-twitch skeletal muscle (3). Cardiac LDA has been shown to be modulated by contractile protein phosphorylation (4–7), as well as by cardiac disease-associated mutations within various contractile proteins (6). In addition, evidence has emerged that the passive force originating from the giant elastic sarcomeric protein titin directly acts to modulate myofilament Ca^{2+} responsiveness (8, 9). Of note, the titin molecule spans the entire half-sarcomere from the Z-disk to the center of the thick filament, and is thus well positioned within the contractile apparatus to relay the mechanical SL input signal (8). The mechanisms underlying the impact of titin strain on myofilament LDA, however, are incompletely understood.

A unifying theory has been advanced whereby the distance between the thin and thick filaments constituting the muscle's sarcomeres is proposed to modulate myofilament Ca^{2+} responsiveness by affecting the probability of cross-bridge formation.

Significance

The Frank–Starling law of the heart represents a fundamental regulatory mechanism whereby cardiac pump performance is directly modulated by the extent of diastolic ventricular filling on a beat-to-beat basis. It is now well established that sarcomere length (SL)-induced changes in cardiac contractile protein responsiveness to activating calcium ions play a major role in this phenomenon. However, the molecular mechanisms that underlie this SL-sensing property are not known. Here, we show by small-angle X-ray diffraction and fluorescent probe techniques that the giant protein titin likely transmits the length signal to induce structural alterations in both thin- and thick-filament contractile proteins. These findings provide insights into the molecular basis of the Frank–Starling regulatory mechanism.

Author contributions: Y.A.-M., K.H., T.C.I., and P.P.d.T. designed research; Y.A.-M., K.H., M.K., and T.C.I. performed research; M.L.G. contributed new reagents/analytic tools; Y.A.-M., K.H., G.P.F., M.K., T.C.I., and P.P.d.T. analyzed data; and Y.A.-M., K.H., T.C.I., and P.P.d.T. wrote the paper.

The authors declare no conflict of interest.

This article is a PNAS Direct Submission.

Freely available online through the PNAS open access option.

[1]Y.A.-M. and K.H. contributed equally to this work.

[2]Present address: Department of Cardiovascular Research, Sidra Medical and Research Center, Doha, Qatar.

[3]Present address: Department of Biology, San Diego State University, San Diego, CA 92182-4614.

[4]Present address: Department of Biological Sciences, University of Massachusetts at Lowell, Lowell, MA 01854; and Department of Physiology and Biophysics, Boston University, Boston, MA 02118.

[5]To whom correspondence should be addressed. Email: pdetombe@luc.edu.

This article contains supporting information online at www.pnas.org/lookup/suppl/doi:10.1073/pnas.1516732113/-/DCSupplemental.

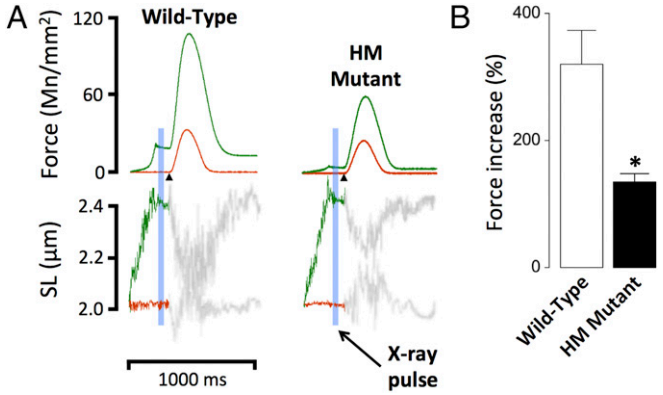

Fig. 1. Impact of titin length on cardiac muscle function. Cardiac muscles were isolated from WT or HM rats and electrically stimulated (arrowheads). (*A*) Force and SL recordings; SL in the diastolic phase was either maintained at SL = 2.0 μm (red) or increased transiently to SL = 2.4 μm (green). (*B*) Average percentage increase of twitch force upon stretch (*$P < 0.05$ WT vs. HM).

Consistent with this notion, analyses of X-ray diffraction patterns obtained from both isolated cardiac and skeletal muscle reveal an inverse relationship between myofilament lattice spacing and SL (10). However, in a multitude of experimental models, we could not find a consistent correlation between myofilament lattice spacing and myofilament Ca^{2+} responsiveness, rendering interfilament spacing a less likely candidate for the molecular mechanism underlying LDA (1). Instead, we obtained experimental evidence suggesting a direct impact of SL on the spread of cooperative activation along the thin filament (11), potentially by modulation of the ordering of myosin heads in relaxed muscle, that is, before electrical activation (12). However, the primary molecular mechanism by which the strain signal is transmitted to the contractile apparatus could not be determined by those studies.

Here, we use a rat model in which a naturally occurring mutation within the splicing factor RBM20 disrupts titin mRNA splicing. One result of this mutation is the cardiac expression of a giant titin isoform in homozygous mutant (HM) animals at all ages (13). The presence of the giant titin isoform in HM myocardium was associated with reduced cardiac passive force upon stretch, as well as a blunted Frank–Starling response and reduced myofilament LDA. Time-resolved small-angle X-ray diffraction revealed stretch-induced conformational structural changes in both thin- and thick-filament contractile proteins during diastole in WT, but not HM, muscles. Our results suggest a prominent contribution of titin strain to the cardiac Frank–Starling mechanism. The mechanism underlying this phenomenon appears not to involve interfilament spacing or movement of myosin heads toward actin in the relaxed muscle but, rather, stretch-induced structural rearrangements in both the thin and thick filaments that is likely directly mediated by titin strain.

Results

Impact on Muscle Function. Fig. 1*A* shows original recordings of twitch force obtained in WT and HM rat myocardium. Muscles were electrically stimulated (Fig. 1*A*, arrowheads) at either short SL (2.0 μm, red) or following stretch to long SL (2.4 μm, green). Just before electrical stimulation, muscles were exposed to a brief X-ray pulse as indicated by the blue bar (Fig. 1*A*). This protocol was repeated 30 times every 10th twitch while a CCD-based X-ray detector recorded the 2D X-ray diffraction pattern (Fig. 2). In both WT and HM rat myocardium, stretch induced an increase in both passive and active twitch force, but the increase was significantly blunted in HM muscles. Fig. 1*B* summarizes the average normalized twitch force increase upon sarcomere stretch. Stretch induced ~320% of baseline twitch force in WT muscles (Fig. 1*B*, open bar), compared with ~134% in HM muscles (Fig. 1*B*, solid bar), demonstrating that reduced titin strain is associated with a significant blunting of the myocardial Frank–Starling mechanism.

Impact on 2D X-Ray Meridional Reflections. Fig. 2*A* shows typical 2D X-ray diffraction patterns recorded at short (*Top*) and long (*Bottom*) SL in WT myocardium. The meridional reflections, which run horizontal in Fig. 2*A*, arise from both thin- and thick-filament proteins, notably myosin (M_1–M_6), troponin (Tn_1–Tn_3), and reflections arising from myosin-binding protein C (Fig. S1). The myosin-binding protein C reflections appear as a series of doublets, possibly the result of interference between the two half-sarcomeres, with each pair (C1, C2, and C4 are visible in our patterns) indexing on an ~44-nm repeat. Stretch induced an apparent increase in some, but not all, meridional reflections, as indicated by the arrows in Fig. 2*A* (*Bottom*). Fig. 2*B* shows the average meridional projections recorded in WT (*Top*, $n = 11$) and HM (*Bottom*, $n = 10$) muscles at short (red) and long (green) SL. Although significant changes in sarcomere structure, as reported by the meridional reflections, were observed in WT muscles, no changes were recorded in HM muscles upon stretch. All measured meridional intensities and periodicities obtained from both groups are summarized in Table S1. On average, the intensity of the second order of myosin-binding protein C ($C_{2,2}$), the second and sixth orders of myosin (M_2 and M_6), and the third order of troponin (Tn_3) increased significantly in intensity upon stretch in WT, but not HM, muscles. Moreover, upon stretch, the periodicity of the M_2 and M_6 myosin reflection, as well as the Tn_3 reflection, significantly increased in WT muscles, but notably not in HM muscles.

Impact on 2D X-Ray Myosin Layer Lines. Fig. 3*A* shows representative first-order myosin layer line projections recorded at short (red) and long (green) SL in WT (*Top*) and HM (*Bottom*) muscles. Fig. 3*A* (*Inset*) also shows a typical 2D X-ray pattern in which the first myosin layer line is delineated by the rectangle (yellow arrow). The radial position of the center of mass of myosin heads can be estimated directly from the position of first-intensity maxima along the layer line; that is, assuming a three-stranded thick filament with helical symmetry, the peak position of the first myosin layer line should correspond to the first maximum of a J3 Bessel function with the argument $2 \bullet \pi \bullet r \bullet R$, where r is a radial reciprocal lattice coordinate and R is the radius to the center of mass of the myosin heads around the thick filament backbone (14). The radial distances of the myosin head to

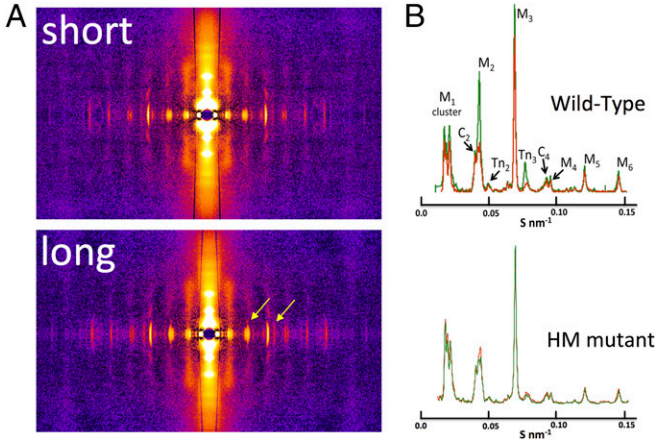

Fig. 2. Two-dimensional X-ray diffraction and meridional analysis. (*A*) Representative 2D X-ray diffraction patterns in WT at short and long SL. Stretch-induced distinct alterations in the meridional reflections (yellow arrows) are shown. (*B*) Average meridional projections at short (red) and long (green) SL. Average intensities and periodicities are summarized in Table S1.

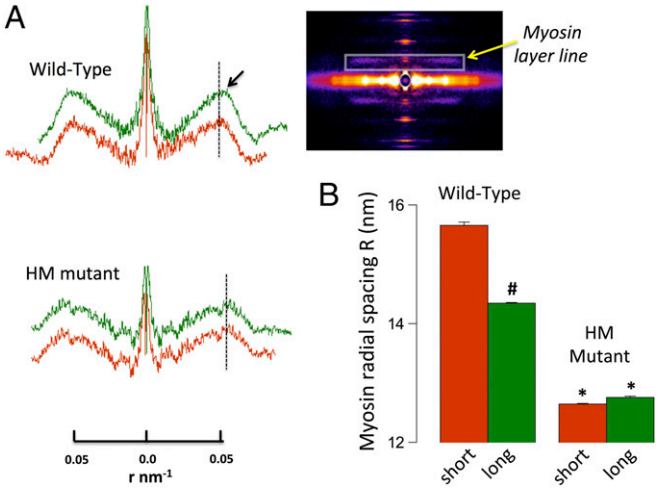

Fig. 3. Myosin layer line analysis. (*A*) Myosin layer line projections in WT and HM muscle at short and long SL scaled to radial spacing r (in nm^{-1}); the black arrow highlights the smaller radial spacing in the WT upon stretch. (*Inset*) Myosin layer line position (yellow arrow). (*B*) Average calculated cross-bridge radial spacing ($^{\#}P < 0.05$ long vs. short; $^{*}P < 0.05$ WT vs. HM).

the thick-filament backbone calculated from these data are summarized in Fig. 3*B*. Overall, the average radial cross-bridge position was ∼19% further away from the thick filament in WT compared with HM muscles. Moreover, sarcomere stretch in WT muscles positioned the myosin head ∼8% closer to the thick filament, whereas no such movement was recorded in the HM muscles.

Impact on Equatorial Reflections. Fig. 4*A* shows average first-order equatorial projections recorded at short (red) and long (green) SL in WT (*Top*) and HM (*Bottom*) muscles. Fig. 4*B* summarizes the average lattice spacing calculated from these reflections (*Top*) and the intensity ratio between the 1,1 and 1,0 planes of symmetry (*Bottom*). Stretch resulted in a reduction in lattice spacing, as reported previously (1), in both groups. Moreover, the average lattice spacing was slightly (∼2%), but significantly, compressed in the HM compared with WT muscles. Likewise, as reported previously (1), the I1,1/I1,0 intensity ratio decreased upon stretch in both muscle groups. Moreover, this ratio was significantly (∼12%) smaller in HM compared with WT muscles. Traditionally, the intensity ratio has been interpreted to indicate mass movement of myosin toward actin (12). However, the current data suggest that interpretation may need to be revisited (see *Discussion*). Finally, although the functional contractile responses and myofilament length-dependent properties of WT and HM myocardium are very different (see Fig. 1, Fig. S2, and Table S2), the responses of both lattice spacing and intensity ratio upon stretch are quite similar overall, indicating that neither parameter correlates with cardiac LDA, as we have reported previously (1, 12). The average equatorial intensities, normalized to the 1,1 intensity (see *Materials and Methods*) recorded in both muscle groups are summarized in Table S3.

Impact on Electron Density Maps. By using phase information estimated from sarcomere structural models (15, 16), we reconstructed radial projection electron density (ED) maps from the first five equatorial reflections of the 2D X-ray diffraction pattern (Table S3; note, a typical 2D X-ray pattern obtained from a WT muscle is shown in Fig. 5, *Bottom Left*). The average ED maps for short (red) and long (green) SL and the difference map between the short and long SL (heat maps; Fig. 5, *Right*), calculated for the WT and HM muscles, are shown in Fig. 5. In WT muscle, stretch induced a significant ($P < 0.01$) increase in the ED of both the thick (7%) and thin (6%) filaments, presumably due to an increase in ordering of both thin and thick filaments around their lattice positions, whereas no significant changes were observed in HM muscles. Moreover, upon stretch, an unidentified ED (peak excess density ∼25% of the peak excess thick-filament backbone density) was observed between the thin (A) and thick (M) filaments in WT muscles, as highlighted by the yellow arrow in the magnified difference map in Fig. 5 (*Bottom Right*). Of note, calculations based on alternative phase assumptions yielded similar relative changes in thick- and thin-filament densities upon stretch: 8% and 6% for thick and thin filaments, respectively, in WT; no significant change in HM; and the appearance of a linking density in WT muscles at long SL that is absent in HM muscle (Fig. S3).

Impact on Recombinant Troponin C Fluorescence. To obtain independent information regarding the structural rearrangement of troponin upon stretch, we used fluorescent probe analysis in chemically permeabilized single myocytes isolated from WT and HM myocardium. Recombinant rat troponin C (TnC) was labeled with the fluorescent probe 5-iodoacetamido-fluorescein (IAF) and partially exchanged for endogenous TnC. In addition, actin was labeled with Alexa-680 phalloidin (Life Technologies, Thermo Scientific) to control for motion artifacts. Fig. 6*A* shows a typical confocal recording of a mechanically attached myocyte; images are shown for the transmission channel (*Top*), red phalloidin (*Middle*), and green TnC (*Bottom*); magnified false red/green color images are shown (*Right*), together with the red/green overlay demonstrating colocalization of the labeled TnC with actin. Fig. 6*B* shows total myocyte TnC fluorescence normalized to the short SL condition as a function of $[Ca^{2+}]$. These data were obtained in the presence of a high concentration of 2,3-butanedione monoxime (50 mM), an agent that blocks strongly bound, force-generating actin–myosin interactions (17). In WT, but not HM, myocytes, stretch induced a significant increase in TnC fluorescence at all $[Ca^{2+}]$. In contrast, increasing $[Ca^{2+}]$ induced a sigmoidal decrease in TnC fluorescence, as has been reported previously for fluorescent probes conjugated to this residue on TnC (18). Of note, the apparent Ca^{2+} sensitivity, as indexed by the EC_{50} parameter, was not affected by sarcomere stretch (Fig. S4); the apparent level of cooperativity, as indexed by the Hill coefficient (19), which was ∼1.0, consistent with biochemical results obtained from isolated TnC or troponin (20), was also not affected. A similar sigmoidal relationship, albeit with a slightly higher Ca^{2+} sensitivity, was observed in the HM myocytes, despite the absence of an impact of stretch in this group. Thus, stretch in WT myocytes induced a conformational

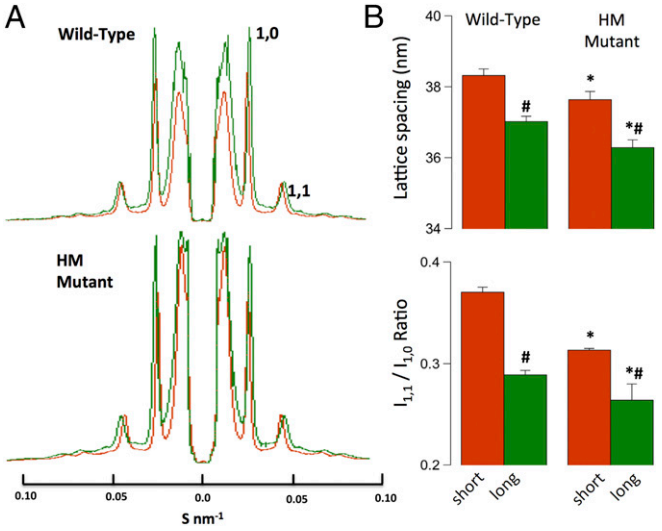

Fig. 4. Equatorial analysis. (*A*) Average equatorial projections scaled to lattice spacing S (in nm^{-1}). (*B*) Average calculated lattice spacings and first-order intensity ratios ($^{\#}P < 0.05$ long vs. short; $^{*}P < 0.05$ WT vs. HM).

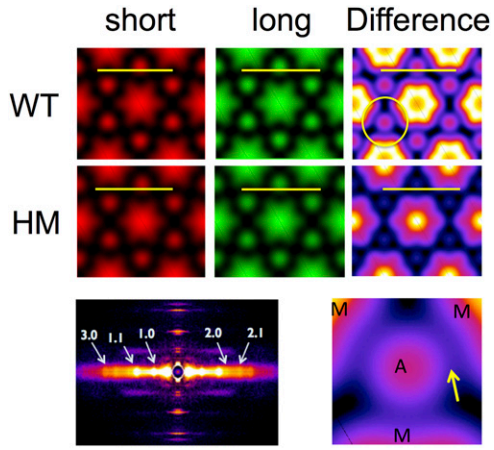

Fig. 5. ED maps. Average radial projection ED calculated from the first five equatorial reflections. A, thin filament; M, thick filament. (Calibration bar, 50 nm.)

rearrangement of troponin, as measured by a florescent probe positioned on TnC, that was distinct from rearrangement of troponin induced by Ca^{2+} ions and that was absent in the HM myocytes.

Discussion

Myofilament Ca^{2+} sensitivity is modulated by SL via an unknown molecular mechanism. Recent evidence has implicated mechanical strain of the giant protein titin in this cellular process (8, 9). Here, we studied isolated cardiac muscle from WT and HM rats expressing a giant titin isoform associated with reduced passive tension, blunted myofilament LDA properties (21), and blunted Frank–Starling responses (9). In WT, X-ray diffraction measurements showed stretch-induced increases in intensity and periodicity of several myosin and troponin reflections, as well as a reduced cross-bridge radius. Moreover, ED reconstruction revealed stretch-induced increased ED at both the thick- and thin-filament positions, and the appearance of an unidentified ED spanning the space between these filaments. The length-dependent changes in structure and function were absent in HM myocardium.

The goal of these studies was to use small-angle X-ray diffraction of intact twitching myocardium from WT and titin mutant rats to investigate the role of changes in sarcomere structure in modulating myofilament LDA. When we initiated these studies, our hypothesis was that analysis of the equator and layer lines would reveal a radially outward movement of myosin heads at longer length indicative of a higher degree of actomyosin interaction in diastole in twitching muscle that we could invoke as part of the molecular explanation for LDA. Our current data conclusively rule out this possibility.

The ratio of the intensities of the 1,1 equatorial reflection to the intensities of the 1,0 reflection, I_{11}/I_{10}, is often used as a measure of the degree of association of cross-bridge mass with the thin filament, usually assumed to be due to a radial shift of mass away from the thick-filament backbone toward the thin filament. Here, we show that the I_{11}/I_{10} ratio is reduced upon sarcomere stretch in both WT and HM myocardium, contrary to our expectation. Interestingly, the I_{11}/I_{10} ratio was lower at both SL in HM compared with WT muscles (Fig. 4*B*), even though, upon stretch, it shows a similar relative change as the change in the WT muscles. Various authors (15, 22) have noted that a decrease in the $I_{1,1}/I_{1,0}$ ratio can be due to a reduced radial ordering of the thin filament relative to the thick filament, such that a decrease in the $I_{1,1}/I_{1,0}$ does not necessarily require radial movement of the cross-bridges, or, alternatively, that it could be due merely to the removal of actin out of the bare zone in the center of the thick filament upon stretch (23). The 2D ED maps calculated from the higher order equatorial data (Fig. 5) indeed show lower density in the thin- and thick-filament positions in HM compared with WT muscles, supporting this notion. The first myosin layer line data can be used to inform on this issue, because they can be more directly interpreted in terms of the radial position of the center of mass of the myosin heads relative to the thick filament. Fig. 3*B* shows that the radius to the center of the myosin heads at the long SL in WT muscles is smaller than at the short SL, consistent with the $I_{1,1}/I_{1,0}$ ratio data shown in Fig. 4. In HM myocardium, however, although the $I_{1,1}/I_{1,0}$ ratio is reduced upon stretch, the centroids of the layer line maxima are unchanged. Moreover, the calculated cross-bridge radius in the HM myocardium is smaller at both short SL and long SL compared with the cross-bridge radius observed in WT myocardium. One should use caution, therefore, in interpreting the $I_{11}/I1_0$ ratio parameter solely in terms of radial motion of myosin heads. These results, along with the evidence from ED maps, suggest that a large part of the lower I_{11}/I_{10} ratio at short SL in both WT and HM myocardium is due to a higher "temperature factor"-type lattice disorder (where the myofilaments occupy a distribution of positions around the expected lattice points), and not to radial movements of myosin heads per se (14). It may also be that the presence of the larger HM titin isoform, and its consequent lower amount of titin-based passive force, reduces the ability of the sarcomere to maintain the myofilaments in the expected lattice positions. Such a phenomenon, by itself, may reduce the probability of productive actomyosin interaction. This hypothesis would be consistent with reported data obtained in animal models, where the presence of a longer than normal isoform of titin in the sarcomere is associated with reduced calcium saturated maximum myofilament force (9, 13, 21, 24), an observation that we confirmed in the present

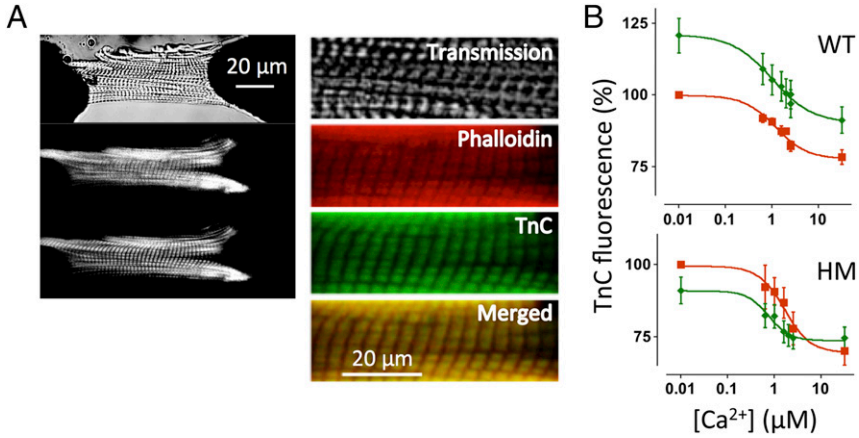

Fig. 6. TnC fluorescence in permeabilized myocytes. (*A*, *Left*) Attached rat permeabilized cardiac myocyte. Transmitted light image (*Top*), Alexa-680 phalloidin image (*Middle*), and TnC-5-iodoacetamido-fluorescein (IAF) image (*Bottom*) are shown. (*A*, *Right*) Expanded scale images also show the red/green merged image. (*B*) TnC fluorescence-$[Ca^{2+}]$ relationships; average EC_{50} parameters are summarized in Fig. S4.

study (Fig. S2 and Table S2). In any case, it is clear that myofilament LDA is not a result of a radial outward movement of myosin heads toward the thin filament upon stretch of the sarcomere in diastole, as we suggested earlier (12).

The M_2 meridional reflection is one of the so-called "forbidden" reflections from the myosin-containing thick filament, because it should not be observed if the thick filament exhibited strict threefold helical symmetry. The existence of forbidden reflections has been attributed to the existence of localized regions on the thick filament with helical tracks containing myosin heads that are distorted from their helical positions. It is premature to attempt a detailed modeling of the structural change upon stretch (and higher titin-based passive tension), but an increase in the M_2 reflection intensity clearly reflects a greater distortion of the helical arrangement of myosin heads, due directly to increased thick-filament strain, or possibly due to interactions between myosin and titin or involvement of myosin-binding protein C.

Stretch induced a significant reduction in the myosin radial spacing in WT, but not HM, muscles. Moreover, in the HM muscles, this parameter was significantly smaller and not affected by stretch (Fig. 3). These results imply that cross-bridges move toward the thick-filament backbone upon diastolic stretch in WT muscles, whereas in HM muscles, cross-bridges are already closer to the thick-filament backbone and, moreover, do not relocate upon stretch. These findings are inconsistent with the notion that myofilament Ca^{2+} sensitivity is regulated by a closer approach of myosin toward actin. The reason why myosin radial spacing is reduced in HM muscles cannot be determined from our study. It is unlikely related to interfilament spacing, because the relative changes in this parameter with changes in SL were similar between the WT and HM muscles (Fig. 4) and, moreover, not correlated to myofilament Ca^{2+} sensitivity at either SL in the HM muscles (Fig. S2 and Table S2).

Stretch of the sarcomere in WT myocardium induced a significant increase in the periodicities of several of the myosin reflections (~0.1–0.3%), and an even larger increase in the apparent periodicity of the Tn_3 reflection (~1.0%). Selective and variable stretch-induced lengthening of the periodicity of some, but not all, X-ray reflections may be an indication that this increase in periodicity is not due to a simple elongation of the underlying sarcomere structure. Rather, it is more likely that this phenomenon is the result of a stretch-induced change in the distribution between various structural states sampled in time by myosin and troponin; that is, stretch may cause a reduction in the mobility of these two protein domains. Such a narrowing of the structural substrate distributions could result in both an increase in the reflection intensity and, simultaneously, a change in its apparent periodicity (Table S1). Of note, a recent X-ray diffraction structural study on tetanized frog skeletal muscle (25) revealed a stress-dependent alteration in myosin periodicity, which was interpreted by those investigators to indicate a redistribution of myosin heads from a folded "OFF" conformation toward an extended "ON" conformation.

The structural rearrangement in troponin upon stretch as reported by the fluorescent probe was distinct from and independent of the structural rearrangement induced by Ca^{2+} activation. It is known that Ca^{2+} binding induces an opening of a hydrophobic patch on TnC with affinity toward the switch peptide domain of TnI, ultimately resulting in release of TnI from the actin-binding site, freeing up the myosin site so as to initiate muscle contraction (26). Hence, it appears that the structural rearrangement of troponin upon stretch is different from the structural rearrangement of troponin induced by Ca^{2+} binding to TnC. Of interest, the apparent binding affinity of TnC for Ca^{2+} was not affected by SL, and there was no indication of cooperativity (19) in this process (Fig. 6 and Fig. S4), in contrast to the relationship between active force development and $[Ca^{2+}]$ (Fig. S2 and Table S2). The implication of this result is that myofilament LDA and the steep cooperativity of myofilament Ca^{2+} activation for force development must be the result of molecular processes downstream of Ca^{2+} binding to TnC. Of interest, stretch of isolated HM permeabilized myocytes to a far greater SL (2.9 μm), where passive force is comparable to passive force seen in WT myocytes at SL = 2.4 μm, induced increased myofilament calcium sensitivity (Fig. S2 and Table S2). These data support the notion that titin mechanical strain contributes to myofilament LDA; furthermore, they demonstrate that myofilament LDA is indeed operational in HM myocardium, albeit only at an extremely long SL, where passive force starts to develop in these myocytes. It should be noted that such an experiment is not feasible in the intact multicellular preparations used here for X-ray diffraction; presence of extracellular elastic structures in those preparations, such as collagen, would resist stretch to such an extreme SL. Moreover, those extracellular structures would likely bear most of the passive force at such extreme SL, placing most of the mechanical strain external to the cardiac sarcomere (8, 9).

In the present study, we compared WT to HM myocardium that was isolated from a rat strain with a spontaneous mutation in the splicing factor RBM20. Although this mutation prominently affects the splicing of titin, it should be noted that this mutation is also known to regulate the splicing of >50 different cardiac muscle proteins (13), including proteins involved in cardiac calcium homeostasis. However, for the purpose of the present study, which focused on diastolic intact multicellular muscles and permeabilized single myocytes, we assumed that the RBM20 mutation only affects titin length within the cardiac sarcomere.

Changes in troponin structure with changes in SL, as suggested by the X-ray results here, point to a mechanism whereby the titin-based strain transmitted by the putative thick/thin-filament bridging structures directly affects the regulatory apparatus promoting productive actomyosin interaction, and hence more force at longer SL. Such a mechanism is also supported by our fluorescent probe findings (Fig. 6), whereby stretch in WT myocytes induced a conformational rearrangement within troponin that was distinct from the conformational rearrangement induced by Ca^{2+} ions and that was, moreover, absent in HM myocytes. In addition, extensive stretch of HM myocytes to an SL, where passive force matched the passive force recorded in the WT myocyte, induced increased myofilament Ca^{2+} sensitivity (Fig. S2 and Table S2), supporting the notion that myofilament LDA is caused by titin-mediated strain and subsequent structural rearrangements within the relaxed thin and thick filaments. What may constitute the molecular mechanism(s) underlying this phenomenon? Our study clearly eliminates closer positioning of myosin heads toward the thin filament (Fig. 3) and decreased interfilament spacing (Fig. 4). Instead, titin strain may be transmitted directly to the thick filament via interactions within the A-band (8, 27) or, alternatively, via interactions between titin and the thin filament within the I-band (28). However, because we found that the troponin and myosin structures are both strain-dependent, our results require that both molecular mechanisms would have to operate simultaneously upon stretch.

An alternative mechanism may be related to the ED we observed bridging the thick and thin filaments upon stretch in WT myocardium (Fig. 5). Because of the low resolution of the reconstruction (~13 nm), it is not possible to determine the chemical identity of this bridging structure directly from our data, and caution should be exercised to not overinterpret this density. The bridging density could simply be due to some of the small number of cycling cross-bridges, known to exist even in diastole (29), special "troponin bridges" linking the thick filament directly to the troponin complex (30, 31), or perhaps to myosin-binding protein C. Myosin-binding protein C is emerging as an important regulator of muscle contraction (27, 32–34). Recent evidence indicates that myosin-binding protein C may activate the thin filament via a direct interaction between its N′ domain and actin and/or tropomyosin (35, 36) that may be strain-dependent. Such a mechanism would explain, in part, the prominent myofilament LDA property of the WT cardiac sarcomere, and the blunting of this property in case of low titin strain (8, 9, 37), the absence of myosin-binding protein C (38, 39), or phosphorylation by protein kinase A (4–7). Although it is not possible, at this time, to identify conclusively the conduits for titin-based strain to

the myofilaments, it is clear that such conduits are necessary to explain the simultaneous thick- and thin-filament structural rearrangements we observed upon stretch, rearrangements that are clearly correlated with increased myofilament calcium sensitivity. It is also clear from our current results that we can conclusively rule out altered interfilament lattice spacing as well as a closer approach of myosin heads toward actin at longer SL as being responsible for myofilament LDA.

Materials and Methods

Right ventricular trabeculae or small papillary muscles were dissected from WT or HM titin mutant rats and mounted in an experimental chamber equipped with a length controller, force transducer, and real-time SL detector. X-ray diffraction experiments were conducted at the BioCAT beamline 18 ID at the Advanced Photon Source, Argonne National Laboratory. Myocytes were prepared from frozen tissue by mechanical homogenization and attached to microneedles situated on an inverted confocal laser-scanning microscope. Detailed methods are provided in *SI Materials and Methods*.

All experimental procedures involving live rats were performed according to institutional guidelines concerning the care and use of experimental animals, and the Institutional Animal Care and Use Committee of the Loyola University Stritch School of Medicine approved all protocols.

ACKNOWLEDGMENTS. We thank Peter Schemmel for assistance with X-ray data analysis. This work was supported, in part, by NIH Grants HL075494 and GM103622. Use of the Advanced Photon Source, an Office of Science User Facility operated for the US Department of Energy (DOE) Office of Science by Argonne National Laboratory, was supported by the US DOE under Contract DE-AC02-06CH11357.

1. de Tombe PP, et al. (2010) Myofilament length dependent activation. *J Mol Cell Cardiol* 48(5):851–858.
2. Mateja RD, de Tombe PP (2012) Myofilament length-dependent activation develops within 5 ms in guinea-pig myocardium. *Biophys J* 103(1):L13–L15.
3. Konhilas JP, Irving TC, de Tombe PP (2002) Length-dependent activation in three striated muscle types of the rat. *J Physiol* 544(Pt 1):225–236.
4. Konhilas JP, et al. (2003) Troponin I in the murine myocardium: Influence on length-dependent activation and interfilament spacing. *J Physiol* 547(Pt 3):951–961.
5. Hanft LM, Biesiadecki BJ, McDonald KS (2013) Length dependence of striated muscle force generation is controlled by phosphorylation of cTnI at serines 23/24. *J Physiol* 591(Pt 18):4535–4547.
6. Sequeira V, et al. (2013) Perturbed length-dependent activation in human hypertrophic cardiomyopathy with missense sarcomeric gene mutations. *Circ Res* 112(11):1491–1505.
7. Kumar M, et al. (2015) Cardiac Myosin-binding Protein C and Troponin-I Phosphorylation Independently Modulate Myofilament Length-dependent Activation. *J Biol Chem* 290(49):29241–29249.
8. Hidalgo C, Granzier H (2013) Tuning the molecular giant titin through phosphorylation: Role in health and disease. *Trends Cardiovasc Med* 23(5):165–171.
9. Methawasin M, et al. (2014) Experimentally increasing titin compliance in a novel mouse model attenuates the Frank-Starling mechanism but has a beneficial effect on diastole. *Circulation* 129(19):1924–1936.
10. Irving TC, Konhilas J, Perry D, Fischetti R, de Tombe PP (2000) Myofilament lattice spacing as a function of sarcomere length in isolated rat myocardium. *Am J Physiol Heart Circ Physiol* 279(5):H2568–H2573.
11. Farman GP, Allen EJ, Schoenfelt KQ, Backx PH, de Tombe PP (2010) The role of thin filament cooperativity in cardiac length-dependent calcium activation. *Biophys J* 99(9):2978–2986.
12. Farman GP, et al. (2011) Myosin head orientation: A structural determinant for the Frank-Starling relationship. *Am J Physiol Heart Circ Physiol* 300(6):H2155–H2160.
13. Guo W, et al. (2012) RBM20, a gene for hereditary cardiomyopathy, regulates titin splicing. *Nat Med* 18(5):766–773.
14. Malinchik S, Xu S, Yu LC (1997) Temperature-induced structural changes in the myosin thick filament of skinned rabbit psoas muscle. *Biophys J* 73(5):2304–2312.
15. Irving TC, Millman BM (1989) Changes in thick filament structure during compression of the filament lattice in relaxed frog sartorius muscle. *J Muscle Res Cell Motil* 10(5):385–394.
16. Fujiwara S, Takezawa Y, Sugimoto Y, Wakabayashi K (2009) Neutron diffraction measurements of skeletal muscle using the contrast variation technique: Analysis of the equatorial diffraction patterns. *J Struct Biol* 167(1):25–35.
17. Farman GP, et al. (2008) Blebbistatin: Use as inhibitor of muscle contraction. *Pflugers Arch* 455(6):995–1005.
18. Putkey JAJ, et al. (1997) Fluorescent probes attached to Cys 35 or Cys 84 in cardiac troponin C are differentially sensitive to Ca(2+)-dependent events in vitro and in situ. *Biochemistry* 36(4):970–978.
19. Rice JJ, Wang F, Bers DM, de Tombe PP (2008) Approximate model of cooperative activation and crossbridge cycling in cardiac muscle using ordinary differential equations. *Biophys J* 95(5):2368–2390.
20. Tachampa K, et al. (2008) Increased cross-bridge cycling kinetics after exchange of C-terminal truncated troponin I in skinned rat cardiac muscle. *J Biol Chem* 283(22):15114–15121.
21. Patel JR, Pleitner JM, Moss RL, Greaser ML (2012) Magnitude of length-dependent changes in contractile properties varies with titin isoform in rat ventricles. *Am J Physiol Heart Circ Physiol* 302(3):H697–H708.
22. Yu LC, Steven AC, Naylor GR, Gamble RC, Podolsky RJ (1985) Distribution of mass in relaxed frog skeletal muscle and its redistribution upon activation. *Biophys J* 47(3):311–321.
23. Matsubara I, Elliott GF (1972) X-ray diffraction studies on skinned single fibres of frog skeletal muscle. *J Mol Biol* 72(3):657–669.
24. Mateja RD, Greaser ML, de Tombe PP (2013) Impact of titin isoform on length dependent activation and cross-bridge cycling kinetics in rat skeletal muscle. *Biochim Biophys Acta* 1833(4):804–811.
25. Linari M, et al. (2015) Force generation by skeletal muscle is controlled by mechanosensing in myosin filaments. *Nature* 528(7581):276–279.
26. Solaro RJ, Kobayashi T (2011) Protein phosphorylation and signal transduction in cardiac thin filaments. *J Biol Chem* 286(12):9935–9940.
27. Pfuhl M, Gautel M (2012) Structure, interactions and function of the N-terminus of cardiac myosin binding protein C (MyBP-C): Who does what, with what, and to whom? *J Muscle Res Cell Motil* 33(1):83–94.
28. Kulke M, et al. (2001) Interaction between PEVK-titin and actin filaments: Origin of a viscous force component in cardiac myofibrils. *Circ Res* 89(10):874–881.
29. Brenner B, Schoenberg M, Chalovich JM, Greene LE, Eisenberg E (1982) Evidence for cross-bridge attachment in relaxed muscle at low ionic strength. *Proc Natl Acad Sci USA* 79(23):7288–7291.
30. Agianian B, et al. (2004) A troponin switch that regulates muscle contraction by stretch instead of calcium. *EMBO J* 23(4):772–779.
31. Perz-Edwards RJ, et al. (2011) X-ray diffraction evidence for myosin-troponin connections and tropomyosin movement during stretch activation of insect flight muscle. *Proc Natl Acad Sci USA* 108(1):120–125.
32. Moss RL, Fitzsimons DP, Ralphe JC (2015) Cardiac MyBP-C regulates the rate and force of contraction in mammalian myocardium. *Circ Res* 116(1):183–192.
33. Previs MJ, Beck Previs S, Gulick J, Robbins J, Warshaw DM (2012) Molecular mechanics of cardiac myosin-binding protein C in native thick filaments. *Science* 337(6099):1215–1218.
34. Sadayappan S, de Tombe PP (2014) Cardiac myosin binding protein-C as a central target of cardiac sarcomere signaling: A special mini review series. *Pflugers Arch* 466(2):195–200.
35. Kampourakis T, Yan Z, Gautel M, Sun Y-B, Irving M (2014) Myosin binding protein-C activates thin filaments and inhibits thick filaments in heart muscle cells. *Proc Natl Acad Sci USA* 111(52):18763–18768.
36. Mun JY, et al. (2014) Myosin-binding protein C displaces tropomyosin to activate cardiac thin filaments and governs their speed by an independent mechanism. *Proc Natl Acad Sci USA* 111(6):2170–2175.
37. Cazorla O, Wu Y, Irving TC, Granzier H (2001) Titin-based modulation of calcium sensitivity of active tension in mouse skinned cardiac myocytes. *Circ Res* 88(10):1028–1035.
38. Cazorla O, et al. (2006) Length and protein kinase A modulations of myocytes in cardiac myosin binding protein C-deficient mice. *Cardiovasc Res* 69(2):370–380.
39. Mamidi R, Gresham KS, Stelzer JE (2014) Length-dependent changes in contractile dynamics are blunted due to cardiac myosin binding protein-C ablation. *Front Physiol* 5:461.
40. Farman GP, Allen EJ, Gore D, Irving TC, de Tombe PP (2007) Interfilament spacing is preserved during sarcomere length isometric contractions in rat cardiac trabeculae. *Biophys J* 92(9):L73–L75.
41. Cingolani HE, Pérez NG, Cingolani OH, Ennis IL (2013) The Anrep effect: 100 years later. *Am J Physiol Heart Circ Physiol* 304(2):H175–H182.
42. Hammersley A (1998) FIT2D *Reference Manual, Version 3.1* (European Synchrotron Radiation Facility, Grenoble, France).
43. Yu LC (1989) Analysis of equatorial x-ray diffraction patterns from skeletal muscle. *Biophys J* 55(3):433–440.
44. Wojdyr M (2010) Fityk: A general-purpose peak fitting program. *J Appl Crytstallogr* 43:1126–1128.
45. Haselgrove JC, Huxley HE (1973) X-ray evidence for radial cross-bridge movement and for the sliding filament model in actively contracting skeletal muscle. *J Mol Biol* 77(4):549–568.
46. Haselgrove JC, Stewart M, Huxley HE (1976) Cross-bridge movement during muscle contraction. *Nature* 261(5561):606–608.
47. Ait Mou Y, le Guennec J-Y, Mosca E, de Tombe PP, Cazorla O (2008) Differential contribution of cardiac sarcomeric proteins in the myofibrillar force response to stretch. *Pflugers Arch* 457(1):25–36.
48. Biesiadecki BJ, Kobayashi T, Walker JS, Solaro RJ, de Tombe PP (2007) The troponin C G159D mutation blunts myofilament desensitization induced by troponin I Ser23/24 phosphorylation. *Circ Res* 100(10):1486–1493.
49. Fan D, Wannenburg T, de Tombe PP (1997) Decreased myocyte tension development and calcium responsiveness in rat right ventricular pressure overload. *Circulation* 95(9):2312–2317.
50. Hawkins CJ, Bennett PM (1995) Evaluation of freeze substitution in rabbit skeletal muscle. Comparison of electron microscopy to X-ray diffraction. *J Muscle Res Cell Motil* 16(3):303–318.
51. Malinchik S, Yu LC (1995) Analysis of equatorial x-ray diffraction patterns from muscle fibers: factors that affect the intensities. *Biophys J* 68(5):2023–2031.